0026-895X/11/7903-499–507$20.00
MOLECULAR PHARMACOLOGY
Vol. 79, No. 3
68551/3665603
Mol Pharmacol 79:499–507, 2011
Printed in U.S.A.

Reactive Oxygen Species-Dependent Apoptosis by Gugulipid Extract of Ayurvedic Medicine Plant *Commiphora mukul* in Human Prostate Cancer Cells Is Regulated by c-Jun N-Terminal Kinase[S]

Dong Xiao, Yan Zeng, Lakshmi Prakash, Vladmir Badmaev, Muhammed Majeed, and Shivendra V. Singh

Department of Pharmacology & Chemical Biology, University of Pittsburgh School of Medicine (D.X., S.V.S.), and University of Pittsburgh Cancer Institute (D.X., S.V.S., Y.Z.), Pittsburgh, PA; and Sabinsa Corporation, Piscataway, New Jersey (L.P., V.B., M.M.)

Received August 31, 2010; accepted November 29, 2010

ABSTRACT

Gugulipid (GL), extract of Indian Ayurvedic medicinal plant *Commiphora mukul*, has been used to treat a variety of ailments. We report an anticancer effect and mechanism of GL against human prostate cancer cells. Treatment with GL significantly inhibited the viability of human prostate cancer cell line LNCaP (androgen-dependent) and its androgen-independent variant (C81) with an IC_{50} of ~1 μM (24-h treatment), at pharmacologically relevant concentrations standardized to its major active constituent z-guggulsterone. The GL-induced growth inhibition correlated with apoptosis induction as evidenced by an increase in cytoplasmic histone-associated DNA fragmentation and sub-G_0/G_1-DNA fraction, and cleavage of poly(ADP-ribose) polymerase. The GL-induced apoptosis was associated with reactive oxygen species (ROS) production and c-Jun NH_2-terminal kinase (JNK) activation. The induction of proapoptotic Bcl-2 family proteins Bax and Bak and a decrease of anti-apoptotic Bcl-2 protein Bcl-2 were observed in GL-treated cells. SV40 immortalized mouse embryonic fibroblasts derived from Bax-Bak double-knockout mice were significantly more resistant to GL-induced cell killing compared with wild-type cells. It is interesting to note that a representative normal prostate epithelial cell line (PrEC) was relatively more resistant to GL-mediated cellular responses compared with prostate cancer cells. The GL treatment caused the activation of JNK that functioned upstream of Bax activation in apoptosis response. The GL-induced conformational change of Bax and apoptosis were significantly suppressed by genetic suppression of JNK activation. In conclusion, the present study indicates that ROS-dependent apoptosis by GL is regulated by JNK signaling axis.

Introduction

Novel strategies for the prevention of prostate cancer are highly desirable because prostate cancer continues to be the leading cause of cancer-related deaths among men in the United States (Whittemore et al., 1995; Jemal et al., 2009). Prostate cancer is usually diagnosed in the sixth or seventh decade of life, which allows a large window of opportunity for intervention to prevent or slow the progression of the disease (Whittemore et al., 1995; Gilligan and Kantoff, 2002). Thus, clinical development of agents from natural products that are relatively safe but can delay the onset and/or progression of human prostate cancer is highly desirable.

Gugulipid (GL), extract of *Commiphora mukul,* has been safely used in the Indian Ayurvedic medicine practice for treatment of different ailments (Badmaev et al., 2003; Urizar and Moore, 2003; Shishodia et al., 2008). Several products of standardized formulations of *C. mukul* are already in human

This work was supported by the National Institutes of Health National Cancer Institute [Grant R21-CA143104].
Article, publication date, and citation information can be found at http://molpharm.aspetjournals.org.
doi:10.1124/mol.110.068551.
[S] The online version of this article (available at http://molpharm.aspetjournals.org) contains supplemental material.

ABBREVIATIONS: GL, gugulipid; CDCFDA, (5-(and-6)-carboxy-2′,7′-dichloroluorescein diacetate, succinimidyl ester; HE, hydroethidine; PARP, poly(ADP-ribose) polymerase; DMSO, dimethyl sulfoxide; DCF, 2′,7′-dichlorodihydrofluorescein; JNK, c-Jun N-terminal kinase; MAPK, mitogen-activated protein kinase; JNKK2, c-Jun N-terminal kinase kinase 2; PrEC, normal human prostate epithelial cell line; ROS, reactive oxygen species; ANOVA, analysis of variance; ERK, extracellular signal-related kinase; MEF, mouse embryonic fibroblast; DKO, double knockout; WT, wild type; NAC, *N*-acetyl cysteine; z-Gug, z-guggulsterone; siRNA, small interfering RNA; CHAPS, 3-[(3-cholamidopropyl)dimethylammonio]propane-sulfonate; mTOR, mammalian target of rapamycin; SV40, simian virus 40.

use as cholesterol-lowering agents (Badmaev et al., 2003; Urizar and Moore, 2003; Shishodia et al., 2008). The z- and E-forms of guggulsterone [4,17(20)-pregnadie-3, 16-dione] have been identified as major active components of GL, which has been used in many clinical trials that have focused on its cholesterol-lowering effect (Badmaev et al., 2003; Urizar and Moore, 2003; Shishodia et al., 2008). Although the antitumor activity of GL has not been studied, the studies, including ours, have shown that z-guggulsterone (z-Gug) inhibits proliferation, induces apoptosis, and suppresses angiogenesis as well as the invasion and metastasis of cancer cells (Gujral et al., 1960; Sinal and Gonzalez, 2002; Urizar et al., 2002; Wu et al., 2002; Badmaev et al., 2003; Cui et al., 2003; Urizar and Moore, 2003; Shishodia and Aggarwal, 2004; Samudio et al., 2005; Singh et al., 2005b, 2007; Cheon et al., 2006; Ichikawa and Aggarwal, 2006; Shishodia et al., 2008; Xiao and Singh, 2008). Apoptosis induction by Gug has been reported in leukemia, multiple myeloma, melanoma, head and neck, lung, ovarian, prostate, and breast cancer cells (Sinal and Gonzalez, 2002; Urizar et al., 2002; Wu et al., 2002; Cui et al., 2003; Shishodia and Aggarwal, 2004; Samudio et al., 2005; Singh et al., 2005b, 2007; Cheon et al., 2006; Ichikawa and Aggarwal, 2006; Xiao and Singh, 2008). We have shown previously that z- and E-Gug inhibit growth of PC-3, DU145, and LNCaP human prostate cancer cells in culture by causing apoptosis (Singh et al., 2005b, 2007). It is noteworthy that a normal prostate epithelial cell line (PrEC) is significantly more resistant to growth inhibition and apoptosis induction by z-Gug compared with prostate cancer cells (Singh et al., 2005b, 2007). The z-Gug-induced cell death in PC-3 cells was not influenced by Bcl-2 protein level but correlated with induction of proapoptotic multidomain Bcl-2 family members Bax and Bak and activation of caspases (Singh et al., 2005b). The z-Gug-induced apoptosis in human prostate cancer cells was initiated by reactive oxygen intermediate-mediated activation of c-Jun NH_2-terminal kinase (Singh et al., 2007). Our previous study demonstrated that z-Gug and E-Gug inhibit angiogenic features (capillary-like tube formation and/or migration) of human umbilical vein endothelial cells and DU145 human prostate cancer cells in vitro at pharmacologically relevant concentrations (Xiao and Singh, 2008). Furthermore, oral gavage of 3 μmol z-Gug to male nude mice (five times per week) inhibits in vivo angiogenesis (Xiao and Singh, 2008).

Based on these data, we hypothesized that GL might be more effective apoptosis-induced in prostate cancer cells because it contains a number of steroids, including the two isomers, z- and E-Gugs (Badmaev et al., 2003; Urizar and Moore, 2003; Shishodia et al., 2008). In the present studies, we tested this hypothesis by examining the effect of GL standardized to z-Gug.

Materials and Methods

Reagents. GL, derived from the gum guggul resin (gum guggul) produced in the soft bark ducts of the *C. mukul* tree, is a registered product of Sabinsa Corporation (Majeed et al., 2002). A manufacturing flow chart for gum guggul resin to GL was described by us previously (Badmaev et al., 2003). Standardization of GL was performed by high-performance liquid chromatography and found to contain ~3.75% z-Gug (Badmaev et al., 2003). The GL was stored at 4°C and found to be stable for at least 6 months. The *z*-Gug was from Steraloids (Newport, RI). Reagents for cell culture including medium, penicillin and streptomycin antibiotic mixture, and fetal bovine serum were purchased from Invitrogen (Carlsbad, CA). The hydroethidine (HE) and 5-(and-6)-carboxy-2′,7′-dichlorofluorescein diacetate, succinimidyl ester (CDCFDA) were from Invitrogen Probes. The enzyme-linked immunosorbent assay kit for quantitation of cytoplasmic histone-associated DNA fragmentation was from Roche Diagnostics (Mannheim, Germany). The p38 MAPK and p44/p42 MAPK (Erk1/2)-targeted small interfering RNA (siRNA) were from Cell Signaling Technology (Danvers, MA). The anti-Bax (6A7) monoclonal antibody was from BD Pharmingen (San Diego, CA), antibodies against Bax (polyclonal anti-Bax), Akt, phosphor-Akt, and phosphor-mTOR were from Cell Signaling Technology, the antibody against α-Tubulin was from Sigma-Aldrich (St. Louis, MO), the antibodies specific for detection of poly(ADP-ribose) polymerase (PARP), Bak, total c-Jun NH_2-terminal kinase (JNK), phospho-(Thr183/Tyr185)-JNK, total p38 MAPK, phospho-(Tyr182)-p38 MAPK, extracellular signal-related kinase 1/2 (ERK1/2), phospho-ERK1/2, and phospho-(Ser63/730)-c-Jun were from Santa Cruz Biotechnology (Santa Cruz, CA), the anti-Bcl-2 antibody was from Dako North America, Inc. (Carpinteria, CA), and anti-actin antibody was from Oncogene Research Products (San Diego, CA). *N*-acetyl-L-cysteine (NAC) was obtained from Sigma-Aldrich.

Cell Culture and Cell Survival Assays. Monolayer cultures of LNCaP and C81 cells were maintained in RPMI 1640 medium supplemented with 10% (v/v) fetal bovine serum, 10 mM HEPES, 1 mM sodium pyruvate, and 0.2% glucose and antibiotics. Normal prostate epithelial cell line PrEC (Lonza Walkersville, Inc., Walkersville, MD) was maintained in PrEBM (Lonza Walkersville, Inc.). The MEFs derived from wild-type and Bax-Bak double-knockout (DKO) mice and immortalized by transfection with a plasmid containing SV40 genomic DNA were generously provided by the late Dr. Stanley Korsmeyer (Dana-Farber Cancer Institute, Boston, MA), and were maintained as described previously (Singh et al., 2005b). Each cell line was maintained in an atmosphere of 95% air and 5% CO_2 at 37°C. The effect of GL and z-Gug on cell viability was determined by colonogenic survival assay and trypan blue dye exclusion assays as described previously (Xiao et al., 2006a, 2008; Kim et al., 2007; Xiao and Singh, 2007). For the colonogenic survival assay, cells (1.5×10^5) were plated in six-well plates for incubation overnight and then were treated with 0.1% DMSO (control group) or 1, 2.5, and 5 μM GL for 24 h. The treated cells were reseeded in six-well plates (500 cells/well) in complete medium without drug. The media were changed every 2 days. After culture for 10 days, the cells were fixed and stained with 0.5% crystal violet in 20% MeOH for colony counting.

Detection of Apoptosis. Apoptosis induction was assessed by analysis of cytoplasmic histone-associated DNA fragmentation, flow cytometric analysis of cells with sub-G_0/G_1 DNA content after staining with propidium iodide, and immunoblotting analysis of cleavage of PARP as described previously (Xiao et al., 2006a; Kim et al., 2007).

Immunoblotting. The cells were treated with GL and were lysed as described previously (Singh et al., 2007; Xiao and Singh, 2008). The lysate proteins were resolved by 6 to 12.5% SDS-polyacrylamide gel electrophoresis and transferred onto membrane. Immunoblotting was performed as described previously (Singh et al., 2007; Xiao and Singh, 2008). The blots were stripped and reprobed with anti-actin antibody to correct for differences in protein loading. Change in protein level was determined by densitometric scanning of the immunoreactive band and corrected for actin loading control. Immunoblotting for each protein was performed at least twice using independently prepared lysates to ensure reproducibility of the results.

ROS Generation Assay. Intracellular ROS generation was measured by flow cytometry after staining with HE and CDCFDA essentially as described previously (Xiao et al., 2008). In brief, 2×10^5 cells were plated in 60-mm culture dishes, allowed to attach by overnight incubation, and exposed to DMSO (control) or desired concentration of GL for specified time intervals. The cells were stained with 2 μM HE and 5 μM CDCFDA for 30 min at 37°C. The cells were collected, and the fluorescence was measured using a Coulter Epics XL Flow

Cytometer. In some experiments, cells were pretreated for specified time periods with NAC (10 mM) before GL exposure and analysis of ROS generation.

Genetic Suppression of JNK in LNCaP Cells. The LNCaP cells were transiently transfected with the plasmid encoding for catalytically inactive mutant of JNK kinase 2 [JNKK2(AA)], a generous gift from Dr. Michael Karin (University of California at San Diego, La Jolla, CA), or empty pcDNA3.1 vector as described previously (Xiao et al., 2008). The cells were then treated with DMSO (control) or 5 μM GL for specified time periods and processed for analysis of DNA fragmentation, immunoblotting for phospho-JNK and phospho-c-Jun or conformational change of Bax.

Analysis of Bax Conformation Change. The cells were treated with 5 μM GL or DMSO (control) for specified time interval and lysed using a solution containing 10 mM HEPES, pH 7.4, 150 mM NaCl, 1% CHAPS, and protease inhibitor cocktail. Aliquots containing 200 μg of lysate proteins were incubated overnight at 4°C with 4 μg of anti-Bax 6A7 monoclonal antibody. Protein G-agarose beads (50 μl; Santa Cruz Biotechnology) were then added to each sample, and the incubation was continued for an additional 2 h at 4°C. The immunoprecipitates were washed five times with lysis buffer and subjected to electrophoresis followed by immunoblotting using polyclonal anti-Bax antibody.

RNA Interference of p38 MAPK and Erk1/2. The cells (1×10^5) were seeded in six-well plates and allowed to attach by overnight incubation. The cells were transfected with 200 nM control nonspecific siRNA or p38 MAPK or Erk1/2-targeted siRNA using Oligofectamine (Invitrogen) according to the manufacturer's recommendations. Twenty-four hours after transfection, the cells were treated with DMSO (control) or 5 μM GL for specified time period. The cells were collected, washed with phosphate-buffered saline, and processed for immunoblotting or analysis of cytoplasmic histone-associated DNA fragmentation as described previously (Xiao et al., 2008; Xiao and Singh, 2010, 2007).

Statistical Analysis. Statistical significance of difference in measured variables between control and treated groups was determined by *t* test or one-way ANOVA. Difference was considered significant at $P < 0.05$.

Results

GL Inhibited Viability of Human Prostate Cancer Cells. The effect of GL standardized to z-Gug on cell viability was determined by the colonogenic assay. By following the colony-formation assaying procedure, the cells were cultured for 10 days after 24-h exposure to GL, and the colony formation (>50 cells/colony) was determined. The viability of both LNCaP and its androgen-independent variant C81 (Fig. 1A) was decreased significantly in a concentration-dependent manner with an IC_{50} for GL of ~1 μM, which is at pharmacologically achievable concentrations (~3 μM; Verma et al., 1999). The growth-inhibitory effect of GL was confirmed by trypan blue dye exclusion assay. Treatment with GL for 24 h resulted in a significant reduction in cell viability in both cells (Fig. 1B). Even though viability of LNCaP and C81 cells was also decreased in the presence of z-Gug (Fig. 1C), the GL seemed relatively more effective compared with z-Gug against both cell lines. Growth-inhibitory effect of GL to the cancer cells was ~10-fold stronger compared with z-Gug (Fig. 1). The results indicate that the anticancer effect of GL against prostate cancer cells is most likely attributable to z-Gug and to other constituent(s). It is noteworthy that a normal prostate epithelial cell line (PrEC) was significantly more resistant to growth inhibition by GL compared with prostate cancer cells (Fig. 1D). For instance, 2.5 μM GL, which inhibited the viability of LNCaP and C-81 cells by approximately 50% (Fig. 1B), had minimal effect on PrEC cell viability (Fig. 1D). These data indicated that human prostate cancer cells, but not normal prostate epithelial cell PrEC, were sensitive to inhibition of cell viability by GL. Because the LNCaP and C81 cells exhibited comparable sensitivity, we can also conclude that androgen-responsiveness is not a critical factor in GL-mediated growth inhibition in prostate cancer cells.

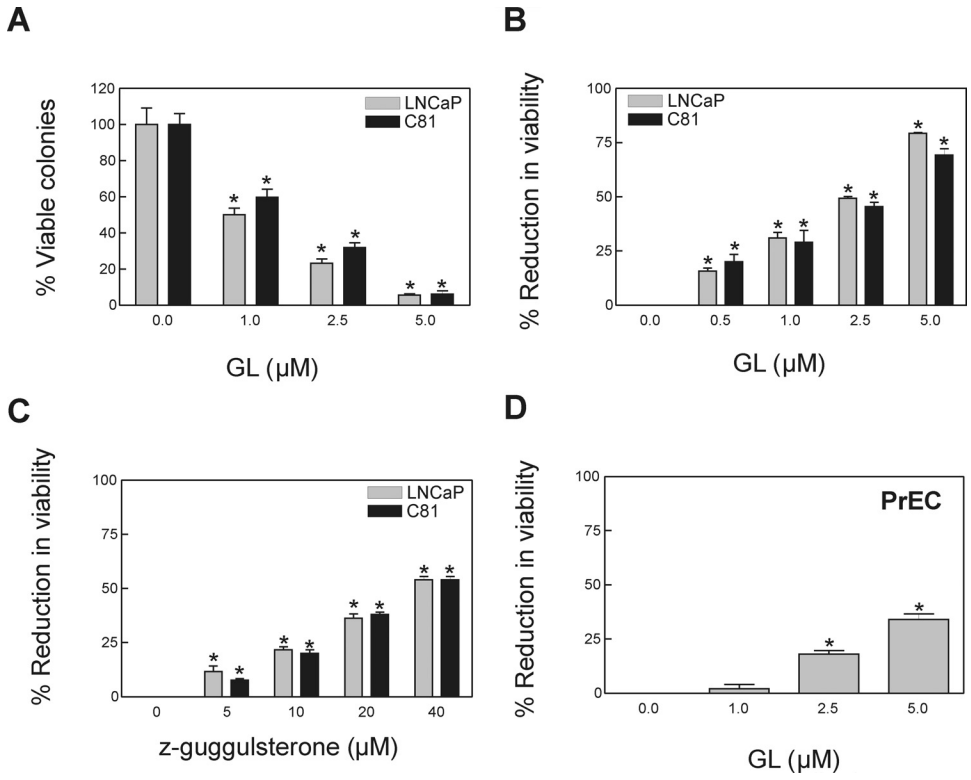

Fig. 1. Effect of GL [GL contains ~3.75% z-Gug and was standardized to z-Gug (micromoles); A, B, and D] and z-Gug (C) on survival of LNCaP, C81, and PrEC cells determined by the colonogenic assay (A) and trypan blue dye exclusion assay (B–D). Cells were treated with different concentrations of GL or z-Gug for 24 h. Columns, mean of three determinations; bars, S.E. *, significantly different ($P < 0.05$) compared with DMSO-treated control by one-way ANOVA followed by Dunnett's test. Similar results were observed in two independent experiments. Representative data from a single experiment are shown.

GL-Mediated Suppression of Cancer Cell Growth Correlated with Apoptotic DNA Fragmentation. To gain further insights into the mechanism of GL-mediated inhibition of prostate cancer cell growth, we determined its effect on cytoplasmic histone-associated DNA fragmentation, a widely used technique for the detection of apoptosis. The GL treatment resulted in a dose-dependent increase in cytoplasmic histone-associated DNA fragmentation in both LNCaP and C81 cells (Fig. 2A). Consistent with cell viability data (Fig. 1D), the PrEC cells were resistant to GL-induced cytoplasmic histone-associated DNA fragmentation (2A). To conform the results of GL-induced apoptotic cell death, we further investigated whether GL treatment increased sub-G_0/G_1 DNA content. A dose-dependent increase in the proportion of cells with sub-G_0/G_1 content was observed in GL-treated LNCaP and C81 cells but not in PrEC compared with DMSO-treated control (Fig. 2B). Furthermore, an immunoreactive band corresponding to cleaved PARP was observed in both cancer cells after treatment with GL (Fig. 2C). Taken together, these observations clearly indicate that the antiproliferative effect of GL against prostate cancer cells was associated with apoptosis induction, and this effect was selective for prostate cancer cells.

GL Treatment Caused ROS Production in Prostate Cancer Cells but Not in a Normal Prostate Epithelial Cell PrEC. Our previous studies have shown that many natural products, such as phenethyl isothiocyanate (Xiao et al., 2006b; Xiao and Singh, 2010), benzyl isothiocyanate (Xiao et al., 2006c, 2008), sulforaphane (Singh et al., 2005a; Xiao et al., 2009), diallyl trisulfide (Xiao et al., 2005b), and z-Gug (Singh et al., 2007) cause apoptosis through the mediation of ROS. We tested whether GL-induced apoptosis was ROS-dependent using flow cytometry after staining with HE and CDCFDA. As can be seen in Fig. 3A, GL-treated C81 cells exhibited a dose- and time-dependent increase in mean DCF fluorescence compared with DMSO-treated (control) cells. For example, the DCF fluorescence in DCF in C81 cells treated for 30 min with 2.5 and 5 μM GL was increased by approximately 7.5- and 3.2-fold compared with control group (Fig. 3A). In time-course experiments, the ROS production was observed as early as 30 min and peaked between 1 and 2 h after exposure (Fig. 3A). The LNCaP cells had almost a same response to GL treatment (Fig. 3B). It is important to note that ROS generation was not determined in the normal prostate epithelial cell PrEC treated with GL (Fig. 3C). These observations clearly indicated that GL treatment resulted in ROS production selectively in human prostate cancer cells.

NAC, an Antioxidant, Attenuated GL-Induced ROS Production and Apoptosis in Prostate Cancer Cells. Next, we designed experiments to determine whether GL-induced ROS generation and apoptotic cell death were attenuated by NAC, an antioxidant. The present results showed that pretreatment with NAC conferred significant protection against GL-induced ROS production and apoptosis in LNCaP cells (Fig. 3D).

Effect of GL Treatment on Levels of Bcl-2 Family Proteins. The Bcl-2 family proteins have emerged as critical regulators of mitochondria-mediated apoptosis by functioning as either promoters (e.g., Bax and Bak) or inhibitors (e.g., Bcl-2 and Bcl-xL) of the cell death process (Chao and Korsmeyer, 1998; Xiao et al., 2004, 2005c). We proceeded to test whether GL-induced apoptosis was regulated by Bcl-2 family proteins. The effect of GL treatment on the levels of Bcl-2 family proteins in LNCaP cells was determined by immunoblotting, and representative blots are shown in Fig. 4A. The levels of multidomain proapoptotic proteins Bax and Bak

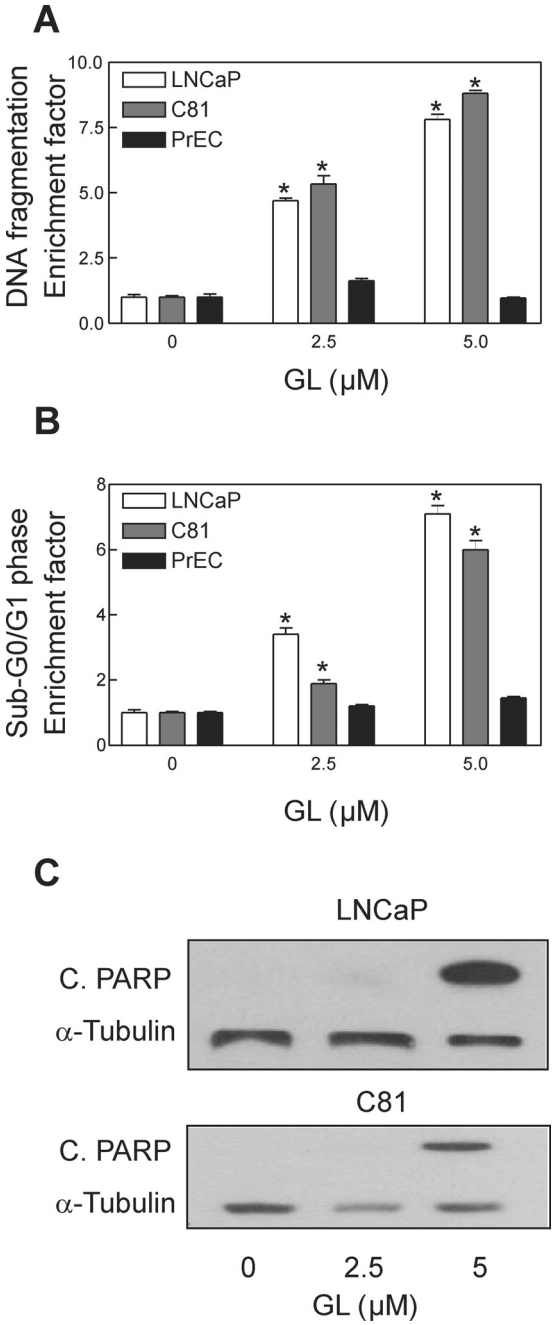

Fig. 2. GL induced apoptosis in LNCaP and C81 cells but not in normal human prostate epithelial cells PrEC, determined by quantitation of cytoplasmic histone associated DNA fragmentation (A), flow cytometry analysis of sub-G_0/G_1 cell phase (B), and immunoblotting cleavage of PARP (C). Cells were treated with the indicated concentrations of GL or DMSO (control) for 24 h. Results in A and B are expressed as enrichment factor relative to cells treated with DMSO (control). Results are mean ± S.E. ($n = 3$). *, significantly different ($P < 0.05$) between the indicated groups by one-way ANOVA followed by Dunnett's test. In C, the cleaved PARP by immunoblotting using lysates from GL-treated or DMSO-treated LNCaP and C81 cells. The blot was stripped and reprobed with anti-α-tubulin antibody to ensure equal protein loading. Similar results were observed in at least two independent experiments. Representative data from a single experiment are shown.

were increased with treatment of LNCaP cells with GL. For example, GL-treated cells for 2 to 24 h resulted in an increase of 2- to 4-fold for Bax and approximately 2-fold for Bak protein expression (Fig, 4A). In addition, the level of antiapoptotic proteins Bcl-2 was significantly decreased on treatment of LNCaP cells with GL (Fig. 4A). However, the expression of Bax proteins was not altered by the same treatment of GL in human normal prostate epithelial cell PrEC (Fig. 4B). These results indicated that GL treatment altered the ratio of proapoptotic to antiapoptotic Bcl-2 family proteins in LNCaP cells.

Bak and Bax Deficiency Conferred Significant Protection against GL-Induced Apoptosis. Because GL treatment increased the Bax and Bak levels in the cancer cells (Fig. 4A), we hypothesized that these proteins might play an important role in the regulation of GL-induced apoptosis. The SV40-immortalized MEFs derived from wild-type (WT) and DKO mice were selected to test the hypothesis. Because of immortalization by transfection with SV40 genomic DNA, the MEFs cannot be regarded as normal fibroblasts. Initially, we used the MEFs from WT and DKO mice to determine the effect of GL treatment on the cleavage of PARP. Similar to LNCaP cells, GL treatment caused a significant increase in the cleavage of PARP in WT MEFs but much less in the DKO MEFs (Fig. 4C). The GL treatment caused concentration-dependent and statistically significant inhibition of cell growth, an increase in apoptotic cells in WT MEFs as judged by trypan blue dye exclusion assays (Fig. 4D), and the analysis of cytoplasmic histone-associated DNA fragmentation (Fig. 4E), respectively. On the other hand, the MEFs derived from DKO MEFs mice were significantly more resistant to GL-induced growth inhibition and cytoplasmic histone-associated DNA fragmentation compared with WT MEFs (Fig. 4, C–E). Together, these results indicated that Bax and Bak play an important role in the execution of GL-induced apoptosis.

GL-Activated JNKs in Human Prostate Cancer Cells but Not in PrEC. We and others have demonstrated previously that z-Gug-induced apoptosis is regulated by JNKs (Singh et al., 2007; Sarfaraz et al., 2008). However, the role of JNK and other MAPK kinases, such as p38-MAPK and ERK in GL-induced apoptosis, has not been studied. To elucidate the mechanism of GL-induced apoptosis in human prostate cancer cells, we investigated its effect on MAPKs. The LNCaP (Fig. 5A) and C81 cells (results not shown) with 5 μM GL exhibited a rapid but sustained activation of JNK for at least 8 h. JNK phosphorylation in GL-treated LNCaP cells could be detected as early as 2 h (1.4-fold compared with the

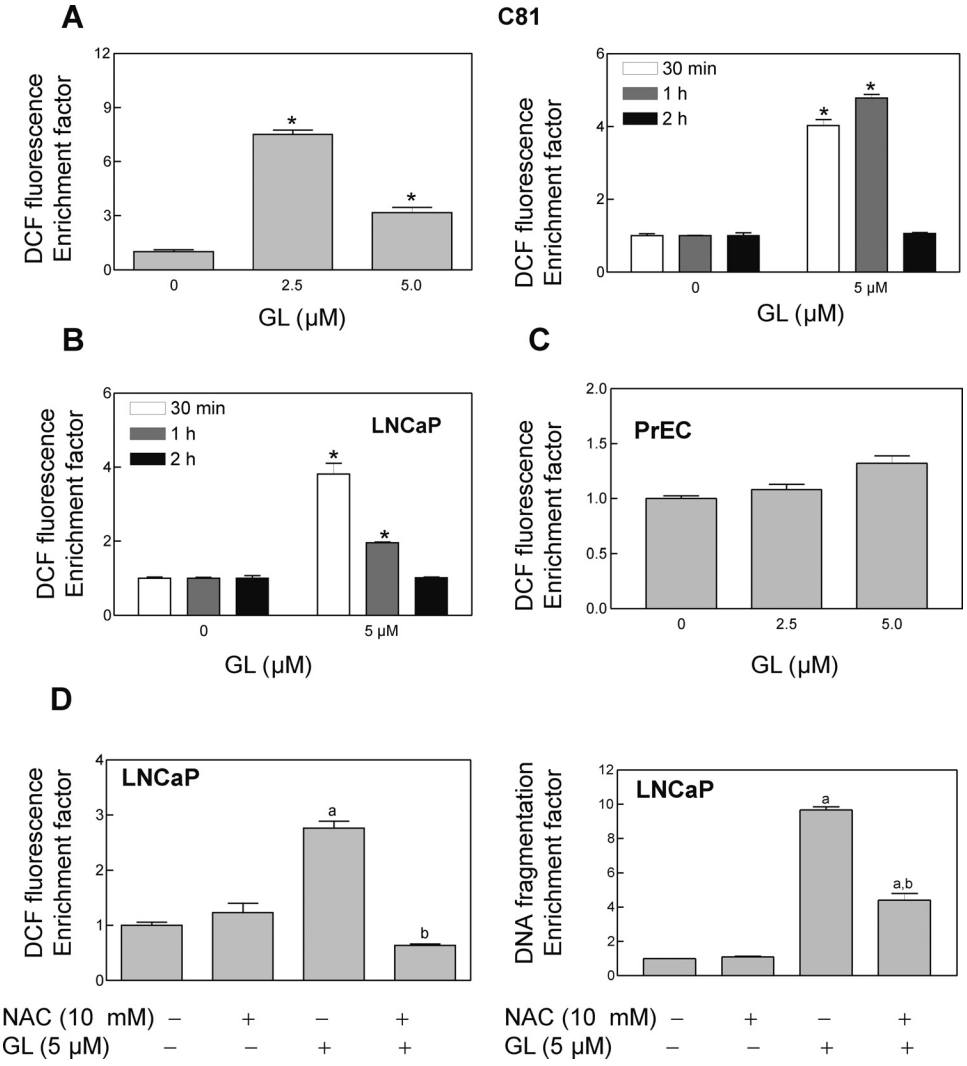

Fig. 3. GL-induced ROS production was involved in apoptotic cell death caused by GL. GL caused ROS generation in C81 (A) and LNCaP (B) cells in dose- (A, left, for C81) and time- (A, right, for C81 and B for LNCaP) dependent manner but not in PrEC (C). D, NAC protected against GL-mediated ROS production and apoptosis. LNCaP cells were treated with 10 mM NAC for 2 h and then exposed to 5 μM GL standardized to z-Gug for 30 min (D, left) or 24 h (D, right). In A to D, results are mean ± S.E. ($n = 3$). *, significantly different ($P < 0.05$) between the indicated groups by one-way ANOVA followed by Dunnett's test (A and C, left) and Bonferroni multiple comparison test (D) and by paired t test (A and B, right). Experiments were repeated twice with triplicate measurements in each experiment. The results were consistent, and representative data from a single experiment are shown.

control cells) after treatment, which was not attributable to an increase in total JNK protein level (data not shown). However, the GL treatment did not activate p38 MAPK and ERK kinases (Fig. 5A) or affected their total protein level (data not shown). In addition, 5 μM z-Gug treatment was not found to activate JNK in LNCaP (Fig. 5A) or C81 (data not shown) cells. We raised the question of whether GL-mediated JNK activation was selective for cancer cells. In contrast to prostate cancer cells, GL did not result in the activation of JNK in normal human prostate epithelial cell PrEC (Fig. 5B). The NAC significantly reduced the phospho-c-Jun (Fig. 5C) protein expression by GL in LNCaP cells. These results indicate that JNK activation mediated by ROS may be involved in GL-induced apoptosis that seemed selective toward prostate cancer cells.

GL-Mediated Activation of Bax Was Inhibited by the Ectopic Expression of JNKK2(AA). The results shown above indicate critical roles of JNK and Bax activation in GL-induced apoptosis but do not provide any insight into the signaling pathways linking these effects. Next, we questioned whether JNK activation contributed to GL-mediated activation of Bax. We addressed this question by determining the effect of ectopic expression of catalytically inactive mutant of JNKK2, which is a JNK-specific upstream kinase (Chen et al., 1998; Singh et al., 2007). GL treatment caused an increase in phosphorylations of JNK and its downstream target c-Jun in the empty vector-transfected LNCaP cells (Fig. 6A). In contrast, GL-mediated hyperphosphorylation of both JNK and c-Jun were fully abolished by the ectopic expression of catalytically inactive JNKK2(AA) in the LNCaP cells (Fig. 6A). In addition, statistically significant increase in cytoplasmic histone-associated DNA fragmentation (6.6-fold of control) resulting from 24-h exposure to GL 5 μM was observed in the empty vector-transfected LNCaP cells but partially and significantly decreased in the cells transiently transfected with JNKK2(AA) (Fig. 6B). Genetic suppression of JNK also attenuated the inhibition of LNCaP cell growth by GL (data not shown). Furthermore, immunoprecipitation analysis of activate Bax from cell lysates was performed by using a monoclonal antibody (6A7) that recognizes an epitope at the N terminus of the active Bax followed by immunoblotting using polyclonal anti-Bax antibody. The GL treatment caused a remarkable increase in Bax conformational change in the empty vector-transfected LNCaP cells (Fig. 6C). More importantly, overexpression of JNKK2(AA) conferred protection against GL-mediated conformational change of Bax (Fig. 6C). Together, these results indicated that the GL-mediated conformational change of Bax was regulated by JNK signaling axis.

However, inhibition of the JNK signaling was not fully protective against the GL-induced cell death (Fig. 6B). Therefore, the roles of the other MAPK signaling such as p38 MAPK and ERK in the apoptosis induction by GL were determined by using the siRNA technology. As can be seen in Supplemental Figs. S1 and S2, the protein levels of p38 MAPK and ERK were knocked down ~50 to 90% by transient transfection of LNCaP cells with p38 MAPK or ERK-targeted siRNA compared with cells transfected with a control non-

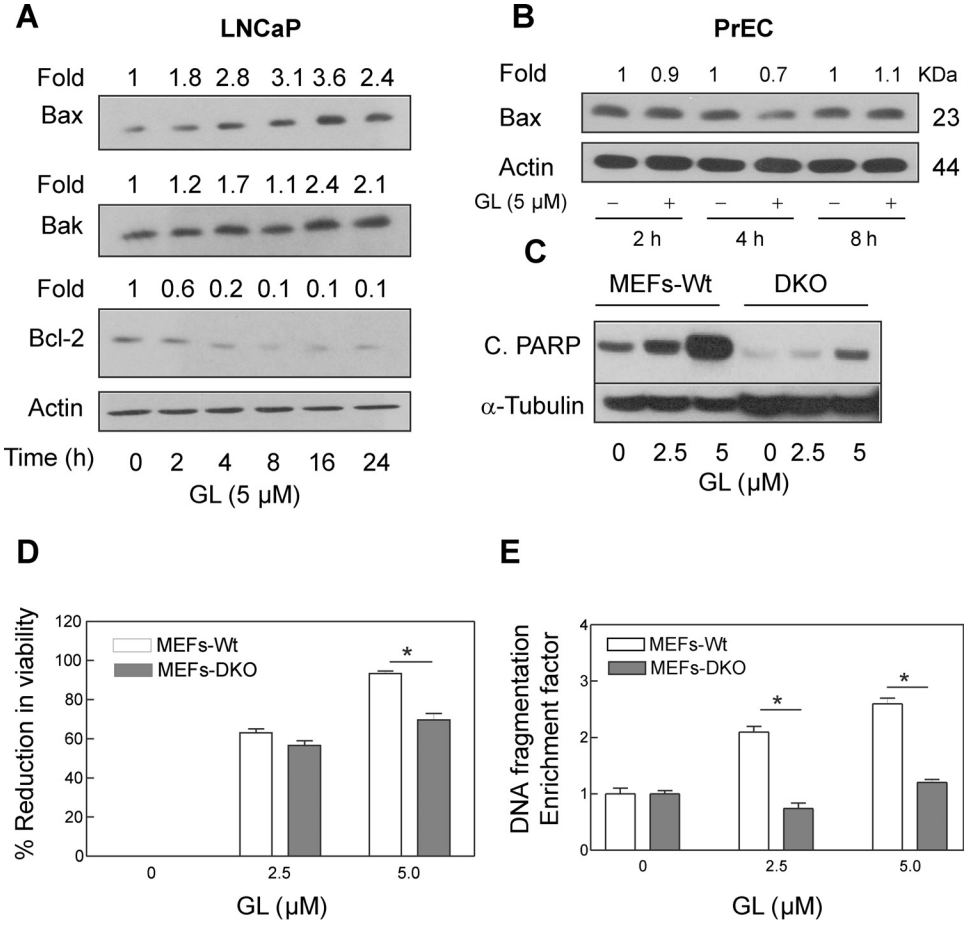

Fig. 4. A, immunoblotting for Bax, Bak, and Bcl-2 proteins using lysates from LNCaP cells treated with DMSO (control) or 5 μM GL standardized to z-Gug for the indicated time periods. B, immunoblotting for Bax protein using lysates from PrEC treated with DMSO (control) or 5 μM GL standardized to z-Gug for the indicated time periods. C, immunoblotting for cleaved PARP protein from the SV40-immortalized mouse embryonic fibroblasts derived WT and Bax and Bak double-knockout mice treated with DMSO (control) or 2.5 and 5 μM GL standardized to z-Gug for 24 h. For A to C, the blots were stripped and reprobed with antiactin antibody to normalize for differences in protein level. The numbers on top of the immunoreactive bands represent a change in protein levels relative to DMSO-treated cells. Immunoblotting for each protein was performed at least twice using independently prepared lysates. The cell survival (D) and cytoplasmic histone-associated DNA fragmentation (E) in LNCaP cells treated with DMSO (control) or 2.5 and 5 μM GL standardized to z-Gug for 24 h. For D and E, columns, mean (n = 3); bars, S.E. *, significantly different ($P < 0.05$) compared with corresponding DMSO-treated control by one-way ANOVA followed by Dunnett's test. Each experiment was performed at least twice with triplicate measurements in each experiment. The results were consistent and representative data from a single experiment are shown.

specific siRNA. However, p38 MAPK-siRNA or ERK-siRNA did not have any protection against the apoptotic cell death induced by GL (Supplemental Figs. S1 and S2). The data indicate that the GL-induced apoptosis is not mediated by p38 MAPK or ERK.

Moreover, we investigated whether Akt signaling was affected in GL-treated LNCaP cells. Exposure of LNCaP cells to GL resulted in a concentration-dependent and significant inactivation of Akt and its substrate mTOR (Fig. 6D). These results suggested that Akt signaling pathway may be involved in the regulation of GL-induced cell death.

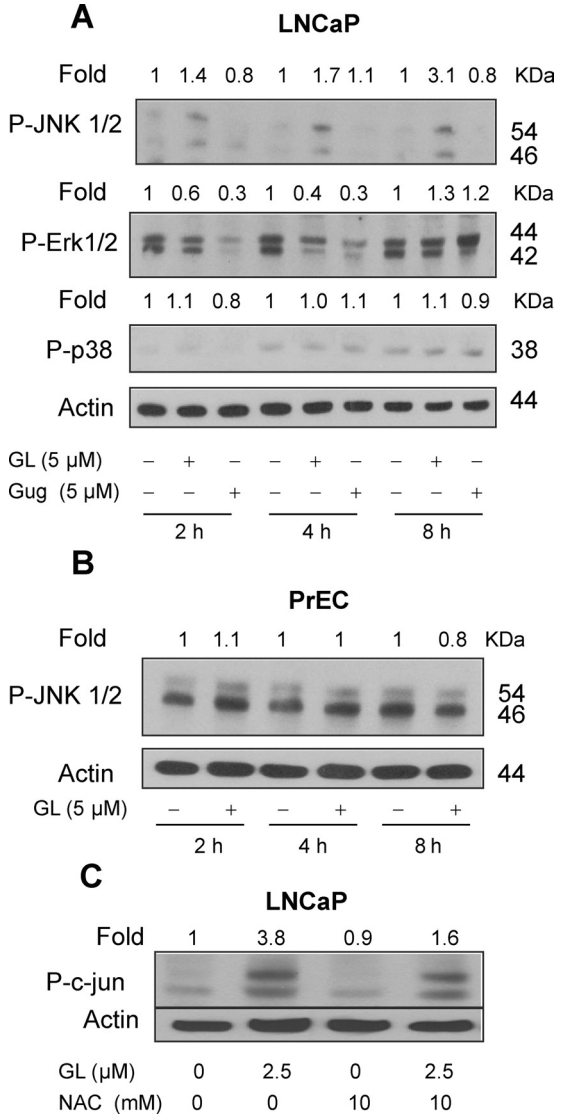

Fig. 5. The GL treatment increased activating phosphorylation of JNK in LNCaP cells, but not in PrEC. Immunoblotting for phospho-JNK, phosphor-Erk, and phospho-p38 MAPK using lysates from LNCaP cells (A) and immunoblotting for phospho-JNK using lysates from PrEC treated with DMSO (control) or 5 μM GL standardized to z-Gug or 5 μM z-Gug for the indicated time periods (B). The blots were stripped and reprobed with anti-actin antibody to ensure equal protein loading. Immunoblotting for each protein was performed twice using independently prepared lysates and the results were similar. Representative data from a single experiment are shown. Fold change in phospho/total protein level relative to DMSO-treated control at each time point is shown on top of the immunoreactive band. C, NAC protected against GL-mediated JNK activation. LNCaP cells were treated with 10 mM NAC for 2 h and then with or without 2.5 μM GL standardized to z-Gug for 8 h. The cellular lysates from these groups were performed for immunoblotting of phospho-c-Jun. The blots were stripped and reprobed with anti-actin antibody to ensure equal protein loading. The numbers on top of the immunoreactive bands represent the change in protein levels relative to corresponding DMSO-treated control. Immunoblotting for the protein was performed twice using independently prepared lysates and the results were similar. Representative data from a single experiment are shown.

Discussion

GL, extract of *C. mukul,* has been safely used for thousands of years in the Indian Ayurvedic medicine practice for treatment of different ailments and has been used recently in many clinical trials focused on its cholesterol-lowering effect (Badmaev et al., 2003; Urizar and Moore, 2003; Shishodia et al., 2008). In the present study, we, for the first time, show that GL has a stronger anticancer potential in human prostate cancer cells as evidenced by the inhibition of cell growth and induction of apoptotic cell death compared with one of its active constituents (z-Gug). Statistically significant inhibition of cell survival by GL was evident at IC_{50} ~1 μM concentrations standardized to z-Gug. The effect on growth inhibition by GL was ~10-fold stronger compared with z-Gug (Fig. 1). It is noteworthy that a normal prostate epithelial cell line PrEC was significantly more resistant to growth inhibition by GL compared with prostate cancer cells. Based on these results, we conclude that GL treatment decreases survival of human prostate cancer cells irrespective of their androgen-responsiveness, a normal prostate epithelial cell line is significantly more resistant to growth inhibition by GL, and uncharacterized constituent(s) of GL may interact additively or synergistically to inhibit the viability of human prostate cancer cells. Even though pharmacokinetic parameters for GL have not been determined in humans, the maximal plasma concentration of z-Gug (C_{max}) in rats was shown to be 3.3 and 18.3 μM after oral gavage with 50 mg z-Gug/kg body weight and intravenous injection with 18 mg z-Gug/kg body weight (Verma et al., 1999). Based on these pharmacokinetic observations, it is possible that the concentrations of GL needed to inhibit cancer cell growth may be achievable in humans. More recently (Leeman-Neill et al., 2009), we reported that treatment with GL (3 μmol standardized to z-Gug, daily for 3 weeks) resulted in the enhancement of cetuximab activity in xenograft model of head and neck cancer.

Apoptosis has emerged as an important mechanism for anticancer effects of many naturally occurring and synthetic agents (Shishodia and Aggarwal, 2004; Samudio et al., 2005; Singh et al., 2005a, 2007; Cheon et al., 2006; Ichikawa and Aggarwal, 2006; Xiao et al., 2006a,c, 2008; Kim et al., 2007; Xiao and Singh, 2007, 2008, 2009, 2010). Our present study indeed indicated that GL inhibits prostate cancer cell viability by causing apoptosis that is characterized by the appearance of cytoplasmic histone-associated DNA fragmentation, subdiploid cells, and cleavage of PARP (Fig. 2). In contrast, PrEC is more resistant to apoptosis induction by GL (Fig. 2). These results clearly indicate that antitumor activity of GL against prostate cancer cells is associated with apoptosis induction.

Tumor-specific induction of oxidative stress is expected to offer a powerful therapeutic modality. In fact, many anticancer agents and naturally occurring and synthetic agents exhibit antitumor activity via ROS-dependent activation of apoptotic cell death (Xiao et al., 2005b,c, 2006b,c; Fang et al., 2007; Kim et al., 2007; Singh et al., 2007). The present results indicate that the cell death caused by GL in human prostate cancer cells is

triggered by ROS generation. This conclusion is based on the following observations: 1) GL treatment caused a dose- and time-dependent ROS production in LNCaP and C81 cells (Fig. 3, A and B); 2) GL-mediated ROS generation and apoptotic cell death was significantly attenuated by antioxidant NAC (Fig. 3D); and 3) the same treatment with GL did not affect the ROS induction (Fig. 3C) and caused apoptotic cell death (Fig. 2, A and B) in PrEC. It was also reported by us (Singh et al., 2007) that ROS is indispensable for z-Gug, one of the important active components of GL, and caused apoptosis in human prostate cancer PC-3 cells.

The proapoptotic Bcl-2 family proteins, which can be subdivided into the Bax subfamily of multidomain proteins (e.g., Bax and Bak) or BH3-only subfamily (e.g., Bid and Bim), induce mitochondrial membrane permeabilization and release of apoptogenic molecules from mitochondria to the cytosol (Singh et al., 2005a; Xiao et al., 2005b,c). An increase in protein levels of Bax and Bak was observed in GL-treated human prostate cancer cells (Fig. 4A), but not in normal prostate epithelial PrEC cell line (Fig. 4B). Furthermore, the SV40-immortalized MEFs derived from Bax- and Bak-DKO mice are statistically significantly more resistant toward GL-induced cell viability and apoptotic cell death compared with MEFs derived from WT mice (Fig. 4, C–E). The present study indicates that the multidomain proapoptotic Bcl-2 family members Bax and/or Bak play a critical role in regulation of GL-induced apoptosis. The GL-induced apoptosis in human prostate cancer cells may be exacerbated because of down-regulation of Bcl-2 (Fig. 4A). Therefore, further studies are needed to determine the role of antiapoptotic Bcl-2 family members, such as Bcl-2 in regulation of GL-mediated cell death in prostate cancer cells.

The involvement of MAPK signaling pathways in carcinogenesis and cancer prevention and therapy is well documented (Xiao et al., 2004, 2005a). An interesting observation of the present study is that GL-induced ROS-dependent apoptosis in our model is regulated by JNK signaling axis (Figs. 5 and 6): we show that 1) GL treatment causes a time-dependent JNK activation in human prostate cancer LNCaP (Fig. 5A) and C81 (date not shown) cells; 2) pharmacological inhibition of JNK confers significant protection against GL-mediated apoptosis in LNCaP and C81 cells (data not shown); 3) GL-induced JNK activation, Bax conformational change (activation) and apoptosis induction were observed in empty vector-transfected LNCaP cells but were inhibited in the cells after ectopic expression of catalytically inactive mutant of JNKK2 (Fig. 6, A–C); and 4) GL treatment could not activate the JNK activation in PrEC (Fig. 5B); JNK was reported to regulate Bax translocation through phosphorylation of Bim (Lei and Davis, 2003) and to promote Bax translocation through phosphorylation of 14-3-3 proteins

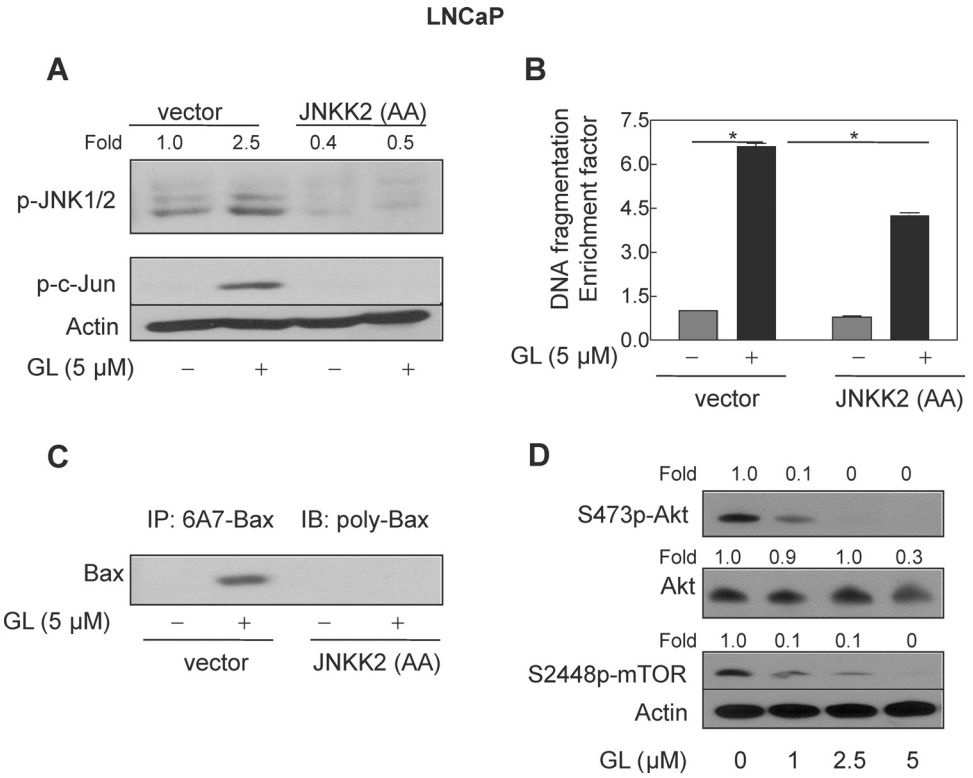

Fig. 6. A, immunoblotting for phospho-JNK and phospho-c-Jun using lysates from LNCaP cells transiently transfected with the empty pcDNA3.1 vector or pcDNA3.1 vector encoding catalytically inactive mutant of JNKK2 [JNKK2(AA)] and treated for 8 h with DMSO (control) or 5 μM GL. B, cytoplasmic histone-associated DNA fragmentation in LNCaP cells transiently transfected with the empty pcDNA3.1 vector or pcDNA3.1 vector encoding JNKK2(AA) and treated for 24 h with DMSO (control) or 5 μM GL. Results are mean ± S.E. ($n = 3$). *, significantly different ($P < 0.05$) between the indicated groups by one-way ANOVA followed by Bonferroni's multiple comparison test. C, analysis of conformational change of Bax using lysates from LNCaP cells transiently transfected with the empty pcDNA3.1 vector or pcDNA3.1 vector encoding JNKK2(AA) and treated for 8 h with DMSO (control) or 5 μM GL. Bax protein was immunoprecipitated from equal amounts of lysate proteins using ant-Bax 6A7 monoclonal antibody. The immunoprecipitated complexes were subjected to immunoblotting using anti-Bax polyclonal antibody. D, immunoblotting for Akt, Ser473-phosphor-Akt, and Ser2448-phospho-mTOR proteins using lysates from LNCaP cells treated with DMSO (control) or indicated concentrations of GL standardized to z-Gug for 24 h. For A and D, the blots were stripped and reprobed with anti-actin antibody to ensure equal protein loading. The numbers on top of the immunoreactive bands represent change in protein levels relative to corresponding DMSO-treated control. Each experiment was repeated twice with comparable results. Representative data from a single experiment are shown.

(Tsuruta et al., 2004; Kim et al., 2006). Thus, it is reasonable to conclude from the present study that GL-inducted Bax activation is regulated by JNK signaling axis. However, it was reported by Sarfaraz et al. that z-Gug-inhibited skin tumorigenesis in SENCAR mice via inhibition of JNK activation. Further studies are needed to systematically explore the role of JNK activation in GL anticancer potential in vivo and other cancers in the future studies. These results indicate also that other MAPK signaling such as p38 MAPK and Erk are not, but the survival signaling Akt may be a mediator for the apoptotic induced by GL.

In conclusion, the present study reveals that GL is a potent inhibitor of prostate cancer cell growth. The GL-mediated antitumor activity is associated with ROS-dependent apoptotic cell death and is regulated by JNK signaling axis.

Acknowledgments

We thank the late Dr. Stanley Korsmeyer for the generous gift of MEFs and Dr. Michael Karin for the generous gift of JNKK2(AA) plasmid.

Authorship Contributions

Participated in research design: Xiao and Singh.

Conducted experiments: Xiao and Zeng.

Contributed new reagents or analytic tools: Prakash, Badmaev, and Majeed.

Performed data analysis: Xiao and Zeng.

Wrote or contributed to the writing of the manuscript: Xiao.

References

Badmaev V, Majeed M, Pacchetti B, and Prakash L (2003) Standardization of *Commiphora mukul* extract in dyslipidemia and cardiovascular disease. *NUTRA Foods* **2:**45–51.

Chao DT and Korsmeyer SJ (1998) BCL-2 family: regulators of cell death. *Annu Rev Immunol* **16:**395–419.

Chen CY, Del Gatto-Konczak F, Wu Z, and Karin M (1998) Stabilization of interleukin-2 mRNA by the c-Jun NH2-terminal kinase pathway. *Science* **280:**1945–1949.

Cheon JH, Kim JS, Kim JM, Kim N, Jung HC, and Song IS (2006) Plant sterol guggulsterone inhibits nuclear factor-κB signaling in intestinal epithelial cells by blocking IκB kinase and ameliorates acute murine colitis. *Inflamm Bowel Dis* **12:**1152–1161.

Cui J, Huang L, Zhao A, Lew JL, Yu J, Sahoo S, Meinke PT, Royo I, Pelaez F, and Wright SD (2003) Guggulsterone is a farnesoid X receptor antagonist in coactivator association assays but acts to enhance transcription of bile salt export pump. *J Biol Chem* **278:**10214–10220.

Fang J, Nakamura H, and Iyer AK (2007) Tumor-targeted induction of oxystress for cancer therapy. *J Drug Target* **15:**475–486.

Gilligan T and Kantoff PW (2002) Chemotherapy for prostate cancer. *Urol* **60:**94–100.

Gujral ML, Sareen K, Tangri KK, Amma MK, and Roy AK (1960) Antiarthritic and anti-inflammatory activity of gum guggul (Balsamodendron mukul Hook). *Indian J Physiol Pharmacol* **4:**267–273.

Ichikawa H and Aggarwal BB (2006) Guggulsterone inhibits osteoclastogenesis induced by receptor activator of nuclear factor-κB ligand and by tumor cells by suppressing nuclear factor-κB activation. *Clin Cancer Res* **12:**662–668.

Jemal A, Siegel R, Ward E, Hao Y, Xu J, and Thun MJ (2009) Cancer statistics, 2009. *CA Cancer J Clin* **59:**225–249.

Kim BJ, Ryu SW, and Song BJ (2006) JNK- and p38 kinase-mediated phosphorylation of Bax leads to its activation and mitochondrial translocation and to apoptosis of human hepatoma HepG2 cells. *J Biol Chem* **281:**21256–21265.

Kim YA, Xiao D, Xiao H, Powolny AA, Lew KL, Reilly ML, Zeng Y, Wang Z, and Singh SV (2007) Mitochondria-mediated apoptosis by diallyl trisulfide in human prostate cancer cells is associated with generation of reactive oxygen species and regulated by Bax/Bak. *Mol Cancer Ther* **6:**1599–1609.

Leeman-Neill RJ, Wheeler SE, Singh SV, Thomas SM, Seethala RR, Neill DB, Panahandeh MC, Hahm ER, Joyce SC, Sen M, et al. (2009) Guggulsterone enhances head and neck cancer therapies via inhibition of signal transducer and activator of transcription-3. *Carcinogenesis* **30:**1848–1856.

Lei K and Davis RJ (2003) JNK phosphorylation of Bim-related members of the Bcl2 family induces Bax-dependent apoptosis. *Proc Natl Acad Sci USA* **100:**2432–2437.

Majeed M, Badmaev V, Bammi RK, Prakash S, and Natarajan S (2002) inventors; Sabinsa Corporation, Sami Chemicals & Extracts (P) Ltd., assignees. Composition and method containing products extracted from Commiphora sp. for prevention and treatment of abnormal cell growth and proliferation in inflammation, neoplasia and cardiovascular disease. U.S. patent 6,436,991. 2002 Aug 20.

Samudio I, Konopleva M, Safe S, McQueen T, and Andreeff M (2005) Guggulsterones induce apoptosis and differentiation in acute myeloid leukemia: identification of isomer-specific antileukemic activities of the pregnadienedione structure. *Mol Cancer Ther* **4:**1982–1992.

Sarfaraz S, Siddiqui IA, Syed DN, Afaq F, and Mukhtar H (2008) Guggulsterone modulates MAPK and NF-kappaB pathways and inhibits skin tumorigenesis in SENCAR mice. *Carcinogenesis* **29:**2011–2018.

Shishodia S and Aggarwal BB (2004) Guggulsterone inhibits NF-kappaB and IkappaBalpha kinase activation, suppresses expression of anti-apoptotic gene products, and enhances apoptosis. *J Biol Chem* **279:**47148–47158.

Shishodia S, Harikumar KB, Dass S, Ramawat KG, and Aggarwal BB (2008) The guggul for chronic diseases: ancient medicine, modern targets. *Anticancer Res* **28:**3647–3664.

Sinal CJ and Gonzalez FJ (2002) Guggulsterone: an old approach to a new problem. *Trends Endocrinol Metab* **13:**275–276.

Singh SV, Choi S, Zeng Y, Hahm ER, and Xiao D (2007) Guggulsterone-induced apoptosis in human prostate cancer cells is caused by reactive oxygen intermediate-dependent activation of c-Jun NH_2-terminal kinase. *Cancer Res* **67:**7439–7449.

Singh SV, Srivastava SK, Choi S, Lew KL, Antosiewicz J, Xiao D, Zeng Y, Watkins SC, Johnson CS, Trump DL, et al. (2005a) Sulforaphane-induced cell death in human prostate cancer cells is initiated by reactive oxygen species. *J Biol Chem* **280:**19911–19924.

Singh SV, Zeng Y, Xiao D, Vogel VG, Nelson JB, Dhir R, and Tripathi YB (2005b) Caspase-dependent apoptosis induction by guggulsterone, a constituent of Ayurvedic medicinal plant *Commiphora mukul*, in PC-3 human prostate cancer cells is mediated by Bax and Bak. *Mol Cancer Ther* **4:**1747–1754.

Tsuruta F, Sunayama J, Mori Y, Hattori S, Shimizu S, Tsujimoto Y, Yoshioka K, Masuyama N, and Gotoh Y (2004) JNK promotes Bax translocation to mitochondria through phosphorylation of 14-3-3 proteins. *EMBO J* **23:**1889–1899.

Urizar NL, Liverman AB, Dodds DT, Silva FV, Ordentlich P, Yan Y, Gonzalez FJ, Heyman RA, Mangelsdorf DJ, and Moore DD (2002) A natural product that lowers cholesterol as an antagonist ligand for FXR. *Science* **296:**1703–1706.

Urizar NL and Moore DD (2003) GUGULIPID: a natural cholesterol-lowering agent. *Annu Rev Nutr* **23:**303–313.

Verma N, Singh SK, and Gupta RC (1999) Pharmacokinetics of guggulsterone after intravenous and oral administration in rats. *Pharm Pharmacol Commun* **5:**349–354.

Whittemore AS, Kolonel LN, Wu AH, John EM, Gallagher RP, Howe GR, Burch JD, Hankin J, Dreon DM, and West DW (1995) Prostate cancer in relation to diet, physical activity, and body size in blacks, whites, and Asians in the United States and Canada. *J Natl Cancer Inst* **87:**652–661.

Wu J, Xia C, Meier J, Li S, Hu X, and Lala DS (2002) The hypolipidemic natural product guggulsterone acts as an antagonist of the bile acid receptor. *Mol Endocrinol* **16:**1590–1597.

Xiao D, Choi S, Johnson DE, Vogel VG, Johnson CS, Trump DL, Lee YJ, and Singh SV (2004) Diallyl trisulfide-induced apoptosis in human prostate cancer cells involves c-Jun N-terminal kinase and extracellular-signal regulated kinase-mediated phosphorylation of Bcl-2. *Oncogene* **23**:5594–5606.

Xiao D, Choi S, Lee YJ, and Singh SV (2005a) Role of mitogen-activated protein kinases in phenethyl isothiocyanate-induced apoptosis in human prostate cancer cells. *Mol Carcinog* **43:**130–140.

Xiao D, Herman-Antosiewicz A, Antosiewicz J, Xiao H, Brisson M, Lazo JS, and Singh SV (2005b) Diallyl trisulfide-induced G_2-M phase cell cycle arrest in human prostate cancer cells is caused by reactive oxygen species-dependent destruction and hyperphosphorylation of Cdc 25 C. *Oncogene* **24:**6256–6268.

Xiao D, Lew KL, Kim YA, Zeng Y, Hahm ER, Dhir R, and Singh SV (2006a) Diallyl trisulfide suppresses growth of PC-3 human prostate cancer xenograft in vivo in association with Bax and Bak induction. *Clin Cancer Res* **12:**6836–6843.

Xiao D, Lew KL, Zeng Y, Xiao H, Marynowski SW, Dhir R, and Singh SV (2006b) Phenethyl isothiocyanate-induced apoptosis in PC-3 human prostate cancer cells is mediated by reactive oxygen species-dependent disruption of the mitochondrial membrane potential. *Carcinogenesis* **27:**2223–2234.

Xiao D, Powolny AA, Antosiewicz J, Hahm ER, Bommareddy A, Zeng Y, Desai D, Amin S, Herman-Antosiewicz A, and Singh SV (2009) Cellular responses to cancer chemopreventive agent D,L-sulforaphane in human prostate cancer cells are initiated by mitochondrial reactive oxygen species. *Pharm Res* **26:**1729–1738.

Xiao D, Powolny AA, and Singh SV (2008) Benzyl isothiocyanate targets mitochondrial respiratory chain to trigger reactive oxygen species-dependent apoptosis in human breast cancer cells. *J Biol Chem* **283:**30151–30163.

Xiao D and Singh SV (2007) Phenethyl isothiocyanate inhibits angiogenesis in vitro and ex vivo. *Cancer Res* **67:**2239–2246.

Xiao D and Singh SV (2008) z-Guggulsterone, a constituent of Indian Ayurvedic medicinal plant *Commiphora mukul*, inhibits angiogenesis in vitro and in vivo. *Mol Cancer Ther* **7:**171–180.

Xiao D and Singh SV (2010) p66Shc is indispensable for phenethyl isothiocyanate-induced apoptosis in human prostate cancer cells. *Cancer Res* **70:**3150–3158.

Xiao D, Vogel V, and Singh SV (2006c) Benzyl isothiocyanate-induced apoptosis in human breast cancer cells is initiated by reactive oxygen species and regulated by Bax and Bak. *Mol Cancer Ther* **5:**2931–2945.

Xiao D, Zeng Y, Choi S, Lew KL, Nelson JB, and Singh SV (2005c) Caspase-dependent apoptosis induction by phenethyl isothiocyanate, a cruciferous vegetable-derived cancer chemopreventive agent, is mediated by Bak and Bax. *Clin Cancer Res* **11:**2670–2679.

Address correspondence to: Dr. Dong Xiao, 2.32b Hillman Cancer Center Research Pavilion, 5117 Centre Avenue, Pittsburgh, PA 15213. E-mail: dongx@upmc.edu